Accepted Manuscript

Intelligent detection of flavor changes in ginger during microwave vacuum drying based on LF-NMR

Yanan Sun, Min Zhang, Bhesh Bhandari, Peiqiang Yang

PII: S0963-9969(19)30106-1
DOI: https://doi.org/10.1016/j.foodres.2019.02.019
Reference: FRIN 8279

To appear in: *Food Research International*

Received date: 30 November 2018
Revised date: 23 January 2019
Accepted date: 8 February 2019

Please cite this article as: Y. Sun, M. Zhang, B. Bhandari, et al., Intelligent detection of flavor changes in ginger during microwave vacuum drying based on LF-NMR, Food Research International, https://doi.org/10.1016/j.foodres.2019.02.019

Intelligent detection of flavor changes in ginger during microwave vacuum drying based on LF-NMR

Yanan Sun[1], Min Zhang[1,2*], Bhesh Bhandari[3], Peiqiang Yang[4]

[1]*State Key Laboratory of Food Science and Technology, Jiangnan University, 214122 Wuxi, Jiangsu, China*

[2]*Jiangsu Province Key Laboratory of Advanced Food Manufacturing Equipment and Technology, Jiangnan University, China*

[3]*School of Agriculture and Food Sciences, University of Queensland, Brisbane, QLD, Australia*

[4] *Suzhou Niumang Analytical Instrument Corporation, 215000 Suzhou, Jiangsu, China*

[*]Corresponding author: Professor Min Zhang

Email: min@jiangnan.edu.cn.

Tel: 0086-(0)510-85807976; Fax: 0086-(0)510-85807976

Abstract

Low-field nuclear magnetic resonance (LF-NMR) and electronic nose combined with Gas chromatography mass spectrometry (GC-MS) were used to collect the data of moisture state and volatile substances to predict the flavor change of ginger during drying. An back propagation artificial neural network (BP-ANN) model was established with the input values of LF-NMR parameters and the output values of sensors for different flavor substances obtained from electronic nose. The results showed that fresh ginger contained three water components: bound water (T_{21}), immobilized water (T_{22}) and free water (T_{23}), with the corresponding peak areas of A_{21}, A_{22} and A_{23}, respectively. During drying, the changes of A_{21} and A_{22} were not significant, while A_{23} and A_{Total} decreased significantly ($p < 0.05$). Linear discriminant analysis (LDA) of electronic nose data showed that samples with different drying time can be well distinguished. Hierarchical clustering analysis (HCA) confirmed that the electronic nose characteristic sensor data S_4, S_5, S_8 and S_{13} corresponded with the data measured by GC-MS. The correlation analysis between LF-NMR parameters and characteristic sensors showed that A_{23} and A_{Total} were significantly correlated with the volatile components ($p < 0.05$). The results of the BP-ANN prediction showed that the model fitted well and had strong approximation ability (R>0.95 and error<3.65%) and stability, which indicated that the ANN model can accurately predict the flavor change during ginger drying based on LF-NMR parameters.

Keyword

Low field nuclear magnetic resonance (LF-NMR), electronic nose, back propagation artificial neural network (BP-ANN) model, flavor, ginger

1. Introduction

Ginger, one of the medicinal and food homologous varieties, is the perennial herbs of the genus Zingiberaceae, and it is also a popular spicy vegetable and seasoning due to its pungent and fragrance, which widely cultivated in Asian, South Africa, North America and Australia (Lu et al., 2018; Zhu et al., 2015). The annual output of ginger in the world is 22 million tons in 2015, of which China produces approximately 10 million tons annually, accounting for 45% of the total global output (Zhu et al., 2015). Ginger is rich in nutrients, including starch, cellulose, protein, amino acids and trace mineral elements (copper, iron, manganese, zinc, chromium, nickel, cobalt), starch accounts for 40%~60%, protein 6.2%~19.8%, total lipid 5.7%~14.5%, cellulose 1.1%~7.0% in terms of dry weight of ginger (Ko et al., 2019; Lu et al., 2018; Si et al., 2017). In addition, the active ingredients of fresh ginger include gingerol, 6-shogaol, curcumin, ginger protease. Therefore, fresh ginger has many functional properties such as anti-oxidation, anti-cancer, anti-neuritis (Srinivasan et al., 2017). Researchers in the field of modern biomedicine are focusing more on the extraction and functional researches of bioactive components in ginger. The change of ginger flavor is mainly related to chemical constituents, which can be divided into gingerol, terpenoid volatile oil and diarylheptanes (Ko et al., 2019; Lu et al., 2018; Choi et al., 2018). The aroma of ginger are related to volatile essential oil, and the pungent taste of ginger mainly depends on gingerol in non-volatile oil (Pang et al., 2017).

The moisture content of fresh ginger is as high as 90%, therefore it is not easy to be stored at room temperature for a long time (Kiran et al., 2013). The quality deterioration of fresh ginger such as water loss, shrinkage, fibrosis and chilling injury is very easy to occur under improper preservation conditions. The annual loss of fresh ginger is up to 20%-40% of total amount due to improper preservation after harvest in China (Zhu et al., 2015). Dehydration is an important technical means for long-term storage of agricultural products (George et al., 2017). Fresh ginger is usually dried mainly by hot air drying, which is easy to operate and requires less investment, but also has the disadvantages of long drying time, low efficiency and poor product quality. In recent years, microwave vacuum drying (MVD) has been widely used in the food industry because of its advantages of faster drying rate, energy saving, convenient operation and being pollution-free (An et al., 2016; Wang et al., 2013; Kubra et al., 2012; Bai-Ngew et al., 2011). The ginger powder can be used not only as condiment or solid beverage, but also as raw material for bread, sweets, biscuits and other foods in order to improve the product nutrition. Meanwhile, the functional extracts of ginger powder can be added to medicinal and health food. Nowadays, the function of dietary therapy and health care has been generally recognized around the world, thus, experts and scholars are paying more and more attention to the comprehensive development and utilization of ginger resources.

Low field nuclear magnetic resonance (LF-NMR) is a fast, accurate, nondestructive and noninvasive method, which uses the spin relaxation properties of hydrogen nucleus in magnetic field to explain the distribution and migration of water

in samples from microscopic point of view. At present, this technique has been successfully applied to study the moisture forms and changes for fruit and vegetable drying process, repeated freezing and thawing process of meat, vacuum cooling process of bean products in recent years. Li et al. (2014) analyzed the distribution and dynamic changes of water components in chicken jerky at different drying temperatures by means of LF-NMR. In order to improve the quality of apple slices and shorten the drying time, Mothibe et al. (2014) studied the effect of ultrasonic and microwave pretreatments on the quality of apple slices, and then the moisture distribution and migration of different pretreatment methods were compared by using LF-NMR. Li et al. (2012) obtained the LF-NMR parameters of defrosted pork under different conditions to study the quality and cooking characteristics. Meanwhile, the chromaticity, shearing force, water holding capacity, pH and related cooking indexes were also measured. The correlation between thawing pork and quality indeces were established by Pearson correlation analysis. The results showed that LF-NMR combined with color analysis could distinguish the water holding capacity of pork under different thawing conditions. Gudjnsdttir et al. (2011) studied the effect of modified atmosphere packaging and salt content on the quality of codfish under refrigerated condition by LF-NMR and traditional quality index determination. The results showed that the higher the salt concentration, the greater the corresponding relaxation time, so the water fluidity of codfish was improved by higher salt concentration.

However, there is limited report on the application of LF-NMR combined with

electronic nose to investigate the relationship between moisture forms and flavor changes of ginger during drying process. Electronic nose is an artificial olfactory recognition technology developed in the 1980s, which used to analyze and identify the overall characteristics of flavor substances. The design principle of electronic nose is equivalent to the mechanism of biological sense of smell. The sensor array in the electronic nose system is equivalent to the nose in the biological system, which can sense different flavor substances and collect the signal information. Then material sensory information is input into the computer, which replaces the brain function in the biological system. The different flavor substances can be distinguished and identified through the software analysis and processing (Liu et al., 2014). The sensor array are consisted by a number of metal oxide sensors, each of which has an interactive sensitivity, an independent sensor does not feel a flavor substance, but a kind of flavor substance.

In this study, the relaxation signals of ginger during MVD were collected, and the water distribution and fluidity under different microwave drying time were studied by LF-NMR. At the same time, the flavor change of ginger during drying was determined by electronic nose and Gas chromatography mass spectrometry (GC-MS). The characteristic sensors of electronic nose were selected through Linear discriminant analysis (LDA) and Hierarchical clustering analysis (HCA). The correlation between LF-NMR parameters and electronic nose feature sensors were analyzed based on Pearson correlation coefficient method. In addition, the flavor prediction models of ginger drying were established by back propagation artificial

neural network (BP-ANN). This study is expected to provide the theoretical basis for intelligence detection of flavor changes quickly and nondestructively, contributing to scientific guidance of the processing and production of dried ginger.

2. Materials and methods

2.1 Sample preparation

Fresh ginger was purchased from the local market in Wuxi and stored in a refrigerator at 4 °C. After cleaning and peeling, the ginger was cut into 1×1×1 cm cube. The 50 g of ginger was placed on a microwave vacuum drying tray and dried with weighing every 10 min for water content at microwave power of 100W, 150W, 200 W, respectively. During the microwave power 200 W drying process, LF-NMR moisture distribution, electronic nose flavor and GC-MS volatile components were measured every 10 min until the moisture content of the dry base was less than 10%. In order to ensure the reliability of the test data, the shape and quality of the samples were as consistent as possible.

2.2 Analysis of test data

2.2.1 Measurement of drying characteristics

The drying curves of ginger sample subjected to MVD was determined following the Li et al., and calculated according to the following equations (Li et al., 2018; Huang et al., 2014).

$$\mathrm{MR} = \frac{M_t - M_e}{M_0 - M_e} \qquad (1)$$

where MR is moisture ratio, M_t is the moisture content at time t, M_e is the equilibrium moisture content, M_0 (g) is the initial moisture content.

In this study, the experimental data were fitted using Page model (as given by Eq. (2))

$MR = \exp(-kt^n)$ (2)

2.2.2 Nuclear magnetic resonance analysis

MesoMR analysis system (main frequency 23 MHz, the coil diameter 60 mm, the magnet temperature 32 °C, and magnet strength 0.5T) was used in the experiment (Lv et al., 2017). Each sample in the process was placed in the linear homogeneous region of the magnet, and signal acquisition was carried out using CPMG (carr-purcell-meiboom-gill) pulse sequence. The T_2 inversion spectrum was obtained by using nuclear magnetic resonance T_2 inversion software. The parameters used in CPMG sequence were set as follows: 90 ° pulse time P1 = 18 μs, 180 ° pulse time P2 = 36μs, sampling point TD = 784794, spectral width SW = 100 kHz, number of echoes Echo Count = 18000, number of repeated scans NS = 4, sampling repetition time TW = 4 000 Ms. During the drying process, 1 g of dried samples were weighed for T_2 acquisition and quality recording. The samples were put into glass tubes of 30 mm diameter, sealed with sealing film to prevent moisture evaporation, and then the samples were put into NMR instrument for analysis and determination to obtain the exponential attenuation spectrum. The signal was collected three times at a time to observe the stability of the signal amplitude. Finally, the inversion spectrum of T_2 was obtained by using the inversion software MultiExp Inv Analysis, and the curve of the effect of MVD on the water state and area of relaxation of ginger were obtained.

2.2.3 E-nose analysis

The ginger samples of different drying group (2.0 g dry basis) were placed in a sealed vial (20 mL) for 60min. The 14 sensors of the electronic nose (iNose; Ruifen Trading Co., Shanghai, China) were used to collect the aroma of each sample and the parameters of the electronic nose were selected based on the machine and the pre-experiment (Chen et al., 2018). The decline trend of the electronic nose aroma curve was very gentle after 150 s. Therefore, the acquisition time was setted at 150 s, which was enough to make the sensor stable. After collecting aroma of each sample, the sensor achieved the "return to zero" effect by cleaning, and the cleaning time was set to 300 s to remove the flavor left by the previous sample. The gas was transferred to the sensor chamber at a flow rate of 1 L min^{-1}.

2.2.4 Volatile compound analysis

The extraction head was aged for 2 h at the inlet of the gas chromatograph and the aging temperature was 250 °C. After 500 mg of crushed ginger sample was sealed in a gas-phase vial, the extractor head of the extractor was immediately inserted into the bottle and balanced at 80 °C for 10 min, then absorbed for 20 min. Finally, the extractor was loaded into the gas chromatography at 250 °C for 5 min, and the instrument was started to collect data. GC and MS conditions were as follows (Wu et al., 2018; Ding et al., 2012):

GC conditions: The Agilent HP-5MS capillary column (30 m×0.25 mm×0.25 μm) was used. The inlet temperature was 250 °C, the carrier gas was He, the column flow rate was 1.0 mL min^{-1}, and the column temperature was programmed (initial temperature was 60 °C, programmed temperature to 116 °C at the rate of 4 °C min^{-1},

kept 20 min, then raised to 160 °C at the rate of 5 °C min^{-1}, and finally ramped up increased to 280 °C at the rate of 20 °C min^{-1} and maintained for 2 min.

MS conditions: EI ion source was adopted with the electronic energy of 70 eV, quadrupole rod temperature of 150 °C and 250 °C interface temperature, the mass range is m/z 50 - 500. Map search: NIST 98 library.

2.3 Artificial Neural Network Modeling

Artificial Neural Network Modeling was performed using MATLAB R2014a (The MathWorks Inc., Natick, MA, USA). Mean Square Error (MSE), coefficient of determination (R^2) of the predicted flavor change were computed to evaluate the performance of fitting and predicting.

2.4 Statistical analysis

Hierarchical clustering analysis (HCA) was conducted using PermutMatrix (Version 1.9.3). HCA was carried out by dividing data into different groups based on similarity or distances between different observational results. Linear discriminant analysis (LDA) of electronic nose sensor was performed using Winmuster Software. LDA is an effective dimensionality reduction approach that maintains most of the information in the original data and assigns each observation to a particular group. In this study, all measurements were performed in triplicate in this study. Statistical analysis was performed using SPSS for Windows (version 21.0 SPSS Inc., Chicago, IL). Data were presented as the mean ± standard error (SE) of determinations made for each sample. Difference among product quality attributes was tested for significance with one-way analysis of variance (ANOVA) followed by Duncan's

multiple-range tests. A 95% confidence level ($p < 0.05$) was used for this purpose.

3. Results and discussion

3.1 Drying characteristics

The drying characteristics of ginger under different vacuum microwave power conditions are shown in Fig 1. With the prolongation of drying time, the moisture content of materials decreased rapidly in the early stage and slowed down in the later stage, but the higher the power, the shorter the time needed to reach the same moisture content. Under the conditions of 100W, 150W and 200W, the drying time recorded were around 110 min, 90 min and 50 min, respectively for the moisture content of ginger reached 10%. As the microwave power increased, the friction and vibration speed between water molecules are accelerated, which promoted the temperature rise. In vacuum environment, the vaporization temperature of water will decrease with the decrease of vapor pressure, which can accelerate the evaporation rate, thus speeding up the drying and shortening the drying time. There are 3 stages of dehydration rates of ginger in the process of MVD, which are acceleration, constant and deceleration stages, respectively (Yasumasa et al., 2019; İlter et al., 2018; Mothibe et al., 2011; Duan et al., 2008). In the acceleration stage, the water in ginger absorbs microwave radiation energy, and the pressure difference of steam increases per unit time caused by discharge of water vapor, then free water is transferred to the surface of the material. This free water on the surface of the material is preferentially heated and evaporated, resulting in faster dehydration rate. In the constant rate stage, the water diffusion rate on the surface of ginger keeps a balance with the internal water

diffusion rate with the evaporation rate. Progressively, the drying of ginger entered the stage of slowing down, the main purpose of this drying stage is to remove the bound water, and the dehydration rate began to decrease gradually. The results are in agreement with those reported by Li et al. (2018) who studied the effect of microwave power on apple drying characteristics using vacuum microwave drying equipment.

3.2 The relaxation characteristics of LF-NMR

The transverse relaxation time T_2 measured by LF-NMR reflects the chemical environment of hydrogen protons in the sample. The relaxation time T_2 becomes shorter, and the peak position on the T_2 spectrum is more closer to the left when the proton is greatly bound (small degree of freedom). T_2 inversion atlas was obtained by multi-exponential fitting of NMR signal data under different drying power for dried ginger. As shown in Fig 2, there were three peaks in the inversion atlas, which were T_{21} (0.1~10 ms), T_{22} (10~100 ms) and T_{23} (100~1000 ms) from left to right. The water molecules of the shortest relaxation time T_{21} was defined as "bound water" (relative content was peak area A_{21}), and this part of water was most closely bound to other molecules, which was considered to be non-rotating "bound" water in magnetic field. The water of relaxation time T_{22} was defined as "semi-bonded water" (relative content is peak area A_{22}), which was second only to the bound water of free water and considered to be able to rotate "bound" water in magnetic field. The water of relaxation time T_{23} had the longest relaxation time (relative peak area A_{23}), which defined as free water, mainly bulk water and structural water. This part of the water has the molecular fluidity of water in aqueous solution and is considered to exist in

vacuoles, protoplasts and intercellular spaces in the cellular structure (Hansen et al., 2010).

As the drying time increased, both T_2 and the area of each peak changed. The size of T_2 reflects the degree of freedom of water in the sample, and the peak area reflects the water content in different states. As can be seen from Fig 2, during the drying process of different time, the change of water content showed a similar trend. First, the peak area decreased gradually, and second, the peak shifted to the left, that is, the free water content decreased continuously, and the combination of water and non-aqueous components was more and more closely linked. The total free water T_{23} decreased significantly ($p < 0.05$) compared with bound water T_{21} and semi-bound water T_{22} during the drying process. In the early stage of drying, A_{23} decreased significantly mainly due to the evaporation of free water, nevertheless A_{21} and A_{22} did not change significantly. A_{Total} represents the total of free water, bound water and semi-free water, and the change trend of that was consistent with the change in A_{23}. In the drying process, free water is gradually removed, resulting in the migration of partially free water to semi bound water. As the drying process proceeds, part of the semi-bound water was bound more closely with the macromolecules, which reduces the degree of freedom of the semi-bound water (Xu et al., 2017). In addition, most of the semi-bound water is transformed into free water and removed, accordingly T_{22} decreased as the drying time prolongs. At the same time, moisture gradient in the material also makes some bound water with relatively high fluidity migrate to semi-bound water (Xiao et al., 2018). The decomposition of nutrients and enzymes in

dried products may also cause partial bound water to migrate to semi-bound water, resulting in a gradual decline of T_{21}. However, due to the low degree of freedom of bound water and semi-bound water, which was more stable in the drying process, the difference of T_{21}, T_{22} was not significant under different time conditions.

3.3 The changes of flavor in drying process

3.3.1 Analysis of changes of volatile components using E-nose

The 14 sensors of the electronic nose represented 14 kinds of flavor substances, as shown in Table 1 (Chen et al., 2018). A radar diagram (Fig. 3) shows the response values of different samples produced by 14 sensors of the electronic nose. All samples with different microwave times presented higher values in sensors S_1, S_2, S_5, S_8 and S_{13}. The trend of similar connection shapes in radar images indicated some similarities between samples treated with different microwave drying times. In addition, all sensors except S_3, S_7, and S_{14} have the largest response distance between fresh ginger and dried products. This indicated that these sensors have made a greater contribution to the flavor differentiation of fresh and dried samples. As can be seen from Fig 3, with the increase of drying time, the response values of most the sensors were gradually decreased, except for S_7 and S_{14}. Their radar diagram almost coincided and only S_{13} had an increasing trend. In the MVD process of ginger, the terpenoids represented by S_2, organic esters represented by S_4 and alcohols represented by S_5 decreased gradually as the drying time prolonged, while the alkenes represented by S_{13} increased gradually. These results suggested that electronic noses have the potential to identify the volatile compounds in different drying stages.

3.3.2 Analysis of changes of volatile components using GC-MS

The volatile flavor compounds in fresh ginger were tested by gas chromatography-mass spectrometry (GC-MS) for the determination of flavor change in ginger during MVD. A total of 58 volatile compounds, mainly alkenes, alcohols aldehydes, ketones and esters, were identified by a combination of NIST 98 library, retention index and related literature comparison. Peak area normalization method was used to quantify each compound. Table 2 presents the composition of volatile components in the drying process of ginger obtained by GC-MS. 51 volatile compounds were detected in fresh ginger, which included 29 alkenes (46.77%), 6 esters (24.43%), 10 alcohols (16.30%), 5 aldehydes (7.61%) and 1 ketone (0.04%). After drying, 41 kinds of volatile compounds were detected, including 22 species of alkenes (56.43%), 3 species of esters (32.23%), 11 species of alcohols (3.37%), and 4 species of aldehydes (4.13%), a ketone (1.05%). Compared with fresh ginger, the volatile components of microwave-dried ginger were significantly reduced ($p < 0.05$), and 10 compounds including 4-carene, 2-carene, germacrene-d, aromadendrene, citronellal, heptyl acetate, L-bornyl acetate, myrtenyl acetate, octyl acetate and (E)-2-decenal were not detected after drying. The possible reason for this effect could be that the cell structure was destroyed and the release of volatile components was increased during the drying process (Munda et al., 2018). In addition, isomerization, degradation and rearrangement reactions of some substances and esterification reactions of alcohols may occur, which can also increase the variety of volatile components in dried ginger (Gong et al., 2004).

The volatile components with higher relative content in fresh ginger were geranyl acetate (22.74%), α-zingberene (14.96%), eucalyptol (10.01%), α-farnesene (7.93%), (E) -citral (7.83%), β-sesquiphellandrene (6.34%), camphene (5.93%) and geraniol (5.96%). These eight components accounted for 81.70% of all the components detected, and were initially identified as the main volatile components of ginger. Eucalyptol has the aroma of camphor, geraniol has the aroma of rose and the content of both decreased with the drying time. Compared with fresh ginger, the relative contents of eucalyptol and geraniol were 0.33% and 0.38%, respectively after 60 min of drying, which were lower than those of fresh ginger slices. For the volatile alkenes components, α-zingerene and α-farnesene have a floral and balsamic aroma, and the content of which was gradually increased with the extension of the drying time. β-sesquiphellandrene and camphene have camphor aroma and the relative contents of these two substances were significantly reduced with the drying time after drying for 30 min. Until 60 min of drying, the relative content was lower than that of fresh ginger. The relative content of geranyl acetate was increased from 22.74% to 28.51% with the extension of drying time, which was consistent with the results reported by Huang et al. (2015). This is probably because the drying process promoted the esterification reaction of alcohols, reducing the content of alcohols and increasing the content of esters. (E)-citral has the aroma of lemon and its relative content increased first and then decreased with the drying time. The relative content was 0.35% after drying for 60 min.

3.4 Discrimination of the flavor by Linear discriminant analysis (LDA) and

Hierarchical clustering analysis (HCA)

LDA analysis is a commonly used dimension reduction technology. Target annotation can make the data points between different categories more distant after projection, and the data points of the same category more compact. Compared with the principal component analysis (PCA) method, which is mainly used to extract the main change information of sample data, LDA is mainly used to classify samples (Kaznowska et al., 2018). The horizontal and vertical coordinates in the LDA analysis diagram represent the contribution rate (weight) of the discriminant function LD1 and LD2 obtained in LDA transformation, respectively. The cumulative contribution rate reflects the reliability of the substitution. The greater the contribution rate, the greater the reliability. The cumulative contribution rate of general requirements is above 70%. The larger the distance between the two samples on the abscissa, the greater the difference.

As can be seen from the Fig 4, the total contribution rate of LDA was 85.9%. The volatile flavor of ginger samples were varied with the increase of drying time. The data collection points of ginger samples with different drying time were located in their respective regions, basically without overlap. The distance between fresh samples and dried samples was the farthest, which indicated that the flavor substances changed during the drying process. There was little difference between the samples dried for 10 min and 20 min, the results showed that the change of flavor was not obvious in the early stage of drying. The distance between fresh samples and samples after 30 min, 40 min and 50 min drying gradually increased, which indicated that the

flavor changed evidently in the middle and late stages of drying. With the prolongation of drying time, the types and contents of volatile substances changed to some extent, but they were generally distributed in the same triangle. Therefore, the e-nose can accurately identify the flavor changes of samples with different drying time.

Fig. 5 showed the HCA results of electronic nose response during MVD of ginger, which adopted the shortest distance method for analysis. The changes of ginger flavor at different drying time can be clustered into four groups, group I consisting of S_8 alone, the e-nose sensor signal value was obviously higher than that of other sensors; group II consisting of S_{13} alone, the change trend of e-nose sensor signal value was completely opposite to that of S_8; group III consisting of S_2, S_4 and S_5, the response values of these sensors had an decreasing trend observably during the drying process, but lower than S_8; the group IV composed of S_1, S_3, S_6, S_7, S_9, S_{10}, S_{11}, S_{12} and S_{14} had no obvious change during drying. The results showed that sensors S_2, S_4, S_5, S_8 and S_{13} were most sensitive to ginger flavor in different drying times. S_2 sensor represents terpenoids and sulphur organic, S_4 sensor represents organic acid esters and terpenes, aromatic compounds, less polar compounds. Therefore, the flavor substance represented by S_2 was contained in S_4, so S_4, S_5, S_8, S_{13} were selected as the characteristic sensor.

3.5 Correlation between E-nose characteristics sensors and NMR parameters

LF-NMR detection can be used as a fast and non-destructive technology to replace the time-consuming detection method if the parameters of NMR have a strong

correlation with the e-nose characteristic sensors. In order to consider the predictability of the whole drying process, Pearson correlation analysis was used to evaluate the relationship between e-nose characteristic sensors (S_4, S_5, S_8, S_{13}) and NMR parameters (A_{21}, A_{22}, A_{23} and A_{Total}) in microwave vacuum-dried ginger cubes. As shown in Table 3, the NMR parameters including A_{23} and A_{Total} were highly positively correlated with each other with high correlation coefficient, whereas not correlated well with A_{21} and A_{22} with low correlation coefficient. Moreover, E-nose characteristic sensor (S_4, S_5, S_8, S_{13}) showed good correlation with NMR parameters. Similarly, S_4, S_5, S_8 also showed a positively correlation with A_{23} and A_{Total} with a correlation coefficient ranging from 0.803 to 0.955. The characteristic sensor of S_{13} showed a negative correlation with A_{23} and A_{Total} with a correlation coefficient -0.803 and -0.954, respectively. These results demonstrated that it could be feasible to monitor the flavor change using LF-NMR during drying process noninvasively.

3.6 Model Establishment and Verification by BP-ANN

In order to establish the prediction model for the change of ginger flavor substances during drying, the echo peak data (A_{21}, A_{22}, A_{23} and A_{Total}) of CPMG attenuation curve were selected as an independent variable X. At the same time, the characteristic sensors S_4, S_5, S_8 and S_{13} of the e-nose were taken as dependent variables Y. BP-ANN method in MATLAB R2014a software was used to construct the prediction model between independent variable X and dependent variable Y. In the process of building the model, 70% of the samples were randomly selected as training set, and the prediction models of S_4, S_5, S_8 and S_{13} established by BP-ANN method

are shown in Fig. 6. As listed in Fig. 6 the predicted values of different samples obtained by BP-ANN method were well correlated with the measured values, and the R of the training set were all greater than 0.97. In order to verify the accuracy and stability of the prediction model, 15% of the samples were used as validation set and 15% as test set. The results showed that the R of the validation set were all greater than 0.93, indicating that the prediction ability of the model was very good. The comprehensive R of the S_4, S_5, S_8 and S_{13} prediction model were 0.9758, 0.9739, 0.9780 and 0.9759, respectively, which showed that the stability of the prediction model were good. The absolute errors between the predicted values and the actual values were small (0.37%, 2.09%, 2.39%, and 3.61%), which indicated that the BP-ANN model can accurately predict the different flavor substances change during ginger drying based on LF-NMR parameters.

Mean Square Error (MSE), coefficient of determination (R^2) of the different flavor prediction models were computed to evaluate the performance of fitting and predicting (Table 4). The larger the R^2, the smaller the MSE, the better the predictive ability of the model. From Table 4, it can be seen that the R^2 of the sensor representing different flavor substances models were greater than 0.94, while the MSE were less than 5×10^{-2}, which indicated that BP-ANN models had excellent predictive ability for ginger flavor during microwave vacuum drying.

4. Conclusions

The free water content monitored by NMR of ginger was significantly reduced, organic acid esters, terpenes, aromatic compounds monitored by e-nose and GC-MS

were significantly reduced and alkenes were increased during microwave vacuum drying. The correlation between the e-nose characteristic sensors (S_4, S_5, S_8, S_{13}) and NMR parameters (A_{21}, A_{22}, A_{23} and A_{Total}) is good. A prediction method using LF-NMR for evaluating changes of flavor substances in ginger during drying process was investigated in this work. The NMR parameters A_{23} and A_{Total} decreased significantly with the prolongation of drying time, which revealed the water fluidity of ginger reduced during drying process, and the loss of water content was mainly caused by the movable or free water. At the same time, there was a good correlation between NMR parameters (A_{21}, A_{22}, A_{23} and A_{Total}) and e-nose characteristic sensors (S_4, S_5, S_8, S_{13}) obtained by LDA and HCA analysis. The results of the prediction model showed that the BP-ANN model can accurately predict the changes of flavor substances in ginger drying process based on NMR parameters. In general, all obtained results demonstrated that LF-NMR technique combined with BP-ANN can be used to monitor flavor changes of ginger during drying in a rapid and nondestructive way.

Conflicts of interest

There are no conflicts of interest to declare.

Acknowledgments

We acknowledge the financial support from National Key R&D Program of China (Contract No. 2017YFD0400901), Jiangsu Province (China) Agricultural Innovation Project(Contract No. CX(17)2017), Jiangsu Province Key Laboratory

Project of Advanced Food Manufacturing Equipment and Technology (No. FMZ201803)，Jiangsu Province(China) “Collaborative Innovation Center for Food Safety and Quality Control”Industry Development Program, National First-class Discipline Program of Food Science and Technology (No. JUFSTR20180205)，all of which enabled us to carry out this study.

References

An, K., Zhao, D., Wang, Z., Wu, J. J., Xu, Y. J., & Xiao, G. S. (2016). Comparison of different drying methods on Chinese ginger (Zingiber officinale Roscoe): Changes in volatiles, chemical profile, antioxidant properties, and microstructure. *Food Chemistry, 197*, 1292-1300.

Bai-Ngew, S., Therdthai, N., & Dhamvithee, P. (2011). Characterization of microwave vacuum-dried durian chips. Journal of Food Engineering, 104(1), 114-122.

Chen, H. Z., Zhang, M., Bhandari, B., & Guo, Z.M. (2018). Evaluation of the freshness of fresh-cut green bell pepper (Capsicum annuum, var. grossum) using electronic nose. *LWT - Food Science and Technology, 87*, 77-84.

Choi, J. G., Kim, S. Y., & Jeong, M. (2018). Pharmacotherapeutic potential of ginger and its compounds in age-related neurological disorders. *Pharmacology & Therapeutics, 182*, 56-69.

Ding, S. H., An, K. J., Zhao, C. P., Li, Y., Guo, Y. H., & Wang, Z. F. (2012). Effect of drying methods on volatiles of Chinese ginger (Zingiber officinale Roscoe). *Food & Bioproducts Processing, 90*(3), 515-524.

Duan, X., Zhang, M., Li, X., & Mujumdar, A. S. (2008). Ultrasonically enhanced osmotic pretreatment of sea cucumber prior to microwave freeze drying. Drying Technology, 26(4), 420-426.

George, J. M., Sowbhagya, H. B., & Rastogi, N. K. (2017). Effect of high pressure pretreatment on drying kinetics and oleoresin extraction from ginger. *Drying*

Technology, 36, 1107-1116.

Gong, F., Fung, Y. S., & Liang, Y. Z. (2004). Determination of volatile components in ginger using gas chromatography–mass spectrometry with resolution improved by data processing techniques. Journal of Agricultural and Food Chemistry, 52 (21), 6378–6383.

Gudjónsdóttir, M., Lauzon, H. L., Magnússon, H., Sveinsdóttir, K., Arason, S., Martinsdóttir, E. et al. (2011). Low field Nuclear Magnetic Resonance on the effect of salt and modified atmosphere packaging on cod (Gadus morhua) during superchilled storage. *Food Research International, 44*(1), 241-249.

Hansen, C. L., Thybo, A. K., Bertram, H. C., Viereck, N., Berg, F., & Engelsen, S. B. (2010). Determination of dry matter content in potato tubers by low-field nuclear magnetic resonance (LF-NMR). *Journal of Agricultural and Food Chemistry, 58*(19), 10300-10304.

Huang, B. K., Wang, G. W., Chu, Z. Y., & Qin, L. P. (2015). Effect of Oven Drying, Microwave Drying, and Silica Gel Drying Methods on the Volatile Components of Ginger (Zingiber officinale Roscoe) by HS-SPME-GC-MS. *International Journal of Food Engineering, 30*(2), 248-55.

Huang, M., Wang, Q., Zhang, M., & Zhu, Q. (2014). Prediction of color and moisture content for vegetable soybean during drying using hyperspectral imaging technology. *Journal of Food Engineering*, 128(1), 24-30.

İlter, I., Akyıl, S., Devseren, E., Okut, D., Koç, M., & Ertekin, F. K. (2018). Microwave and hot air drying of garlic puree: drying kinetics and quality

characteristics. *Heat & Mass Transfer, 54*(10), 2101-2112.

Kaznowska, E., Depciuch, J., Łach, K., Kołodziej, M., Koziorowska, A., Vongsvivut, J., Zawlik, I., Cholewa, M., & Cebulski, J. (2018). The classification of lung cancers and their degree of malignancy by FTIR, PCA-LDA analysis, and a physics-based computational model. *Talanta, 186*, 337-345.

Kiran, C. R., Chakka, A. K., & Amma, K. P. P. (2013). Influence of Cultivar and Maturity at Harvest on the Essential Oil Composition, Oleoresin and [6]-Gingerol Contents in Fresh Ginger from Northeast India. Journal of Agricultural & Food Chemistry, 61(17), 4145-4154.

Ko, M. J., Nam, H. H., & Chung, M. S. (2019). Conversion of 6-gingerol to 6-shogaol in ginger (Zingiber officinale) pulp and peel during subcritical water extraction. *Food chemistry, 270*, 149-155.

Kubra, I. R., & Rao, L. J. M. (2012). Effect of microwave drying on the phytochemical composition of volatiles of ginger. *International Journal of Food Science and Technology, 47*(1), 53-60.

Li, C. B., Liu, D. Y., Zhou, G. H., Xu, X. L., Qi, J., Shi, P. L. et al. (2012). Meat quality and cooking attributes of thawed pork with different low field NMR T_{21}. *Meat Science, 92* (2), 79-83.

Li, L., Zhang, M., Bhandari, B., & Zhou, L. (2018). LF-NMR online detection of water dynamics in apple cubes during microwave vacuum drying. *Drying Technology, 36*, 2006-2015.

Li, M. Y., Wang, H. B., Zhao, G. M., Qiao, M. W., Li, M., Sun, L. X., et al. (2014).

Determining the drying degree and quality of chicken jerky by LF-NMR. *Journal of Food Engineering, 139* (139), 43-49.

Liu, F., Song, S., Zhang, X., Tan, C., & Karangwa, E. (2014). Effect of sterilization methods on ginger flavor beverage assessed by partial least squares regression of descriptive sensory analysis and gas chromatography–mass spectrometry. *European Food Research and Technology, 238*(2), 247-257.

Lu, M. W., Cao, Y., Xiao, J., Song, M. Y., & Ho C. T. (2018). Molecular mechanisms of the anti-obesity effect of bioactive ingredients in common spices: a review. *Food & Function, 9*, 4569-4581.

Lv, W. Q., Zhang, M., Bhandari, B., Li, L. L., & Wang, Y. C. (2017). Smart NMR Method of Measurement of Moisture Content of Vegetables During Microwave Vacuum Drying. *Food Bioprocess Technology, 10*, 2251-2260.

Mothibe, K. J., Zhang, M., Mujumdar, A. S., Wang, Y. C., & Cheng, X. F. (2014). Effects of Ultrasound and Microwave Pretreatments of Apple Before Spouted Bed Drying on Rate of Dehydration and Physical Properties. *Drying Technology, 32* (15), 1848-1856.

Mothibe, K. J., Zhang, M., Nsor-Atindana, J., & Wang, Y. C. (2011). Use of ultrasound pretreatment in drying of fruits: drying rates, quality attributes, and shelf life extension. Drying Technology, 29(14), 1611-1621.

Munda, S., Dutta, S., Haldar, S., & Lal, M. (2018). Chemical Analysis and Therapeutic Uses of Ginger (Zingiber officinale Rosc.) Essential Oil: A Review. *Journal of Essential Oil Bearing Plants, 21*, 994-1002.

Pang, X., Cao, J., Wang, D., Qiu, J., & Kong, F. Y. (2017). Identification of Ginger (Zingiber officinale Roscoe) Volatiles and Localization of Aroma-Active Constituents by GC-Olfactometry. *Journal of Agricultural and Food Chemistry, 65*(20), 4140-4145.

Si, W., Chen, Y.P., Zhang, J., Chen, Z.Y., & Chung, H.Y. (2017) Antioxidant activities of ginger extract and its constituents toward lipids. *Food Chemistry*, 239:1117-1125.

Srinivasan, K. (2017). Ginger rhizomes (Zingiber officinale): A spice with multiple health beneficial potentials. *Pharma Nutrition, 5*(1), 18-28.

Wang, Y., Zhang, M., Mujumdar, A. S., Mothibe, K. J., & Roknul Azam, S. M. (2013). Study of drying uniformity in pulsed spouted microwave–vacuum drying of stem lettuce slices with regard to product quality. *Drying Technology*, 31(1), 91-101.

Wu, X. F., Zhang, M., Bhandari, B., & Li, Z. Q. (2018). Effects of microwave-assisted pulse-spouted bed freeze-drying (MPSFD) on volatile compounds and structural aspects of Cordyceps militaris. *Journal of the Science of Food & Agriculture*, 0-0.

Xiao Q. (2018). Drying process of sodium alginate edible films forming solutions studied by LF-NMR. *Food Chemistry, 250*, 83-88.

Xu, F. F., Jin, X., Zhang, L., & Chen, X. D. (2017). Investigation on water status and distribution in broccoli and the effects of drying on water status using NMR and MRI methods. *Food Research International, 96*, 191-197.

Yasumasa, A., Shoji, H., Hiroshi, N., Itaru, S., Tomoya, O., Hiroshi, O., et al. (2019).

Effects of prefreezing on the drying characteristics, structural formation and mechanical properties of microwave-vacuum dried apple. Journal of Food Engineering, 244, 170-177.

Zhu, D. S., Liu, R. B.., Du, W., Ge, Y. H., Cao, X. H., & Li, J. R. (2015). Research progress in ingredient difference among different types of ginger and the postharvest preservation technology. *Science and Technology of Food Industry*, 36, 375-378.

Figure and table captions

Fig. 1. Effect of microwave power (100, 150 and 300 W) on drying curves for ginger cubes during MVD: Moisture ratio vs. Drying time (drying temperature 60 °C).

Fig. 2. The transverse relaxation time (T_2) curves of the ginger cubes during MVD under 200 W microwave power.

Fig. 3. Radar chart of E-nose analysis of flavor of ginger under 200 W microwave power.

Fig. 4. Linear Discriminant Analysis (LDA) chart of E-nose analysis of flavor of ginger.

Fig. 5. Hierarchical clustering analysis (HCA) chart of E-nose sensors analysis of flavor of ginger.

Fig. 6. Establishment of prediction model by BP-ANN. (a) The prediction model of organic acid esters and terpenes (S_4); (b) The prediction model of alcohol (S_5); (c) The prediction model of nitrogen oxides (S_8); (d) The prediction model of alkenes (S_{13}).

Table 1. Properties of sensor on MOS electronic nose.

Table 2. The volatile compounds of ginger with different drying times as detected by GC-MS.

Table 3. Correlation analysis between electronic nose sensors and NMR parameters.

Table 4. Performance of different flavor prediction models

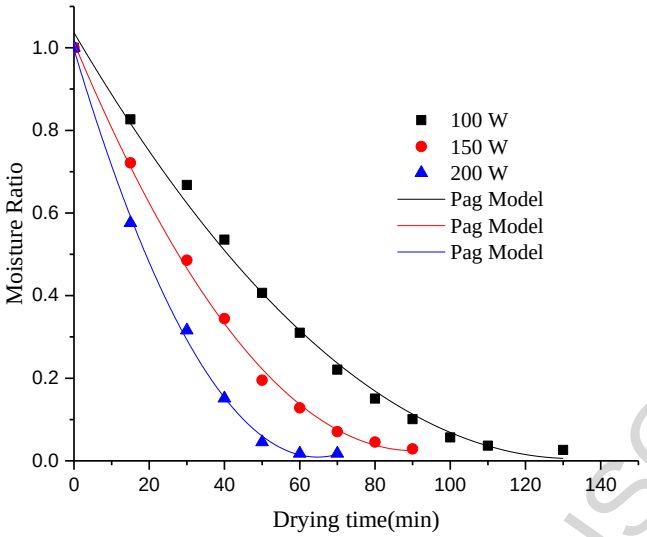

Fig 1. Effect of microwave power on drying curves for ginger cubes during MVD: Moisture ratio vs. Drying time (drying temperature 60 °C).

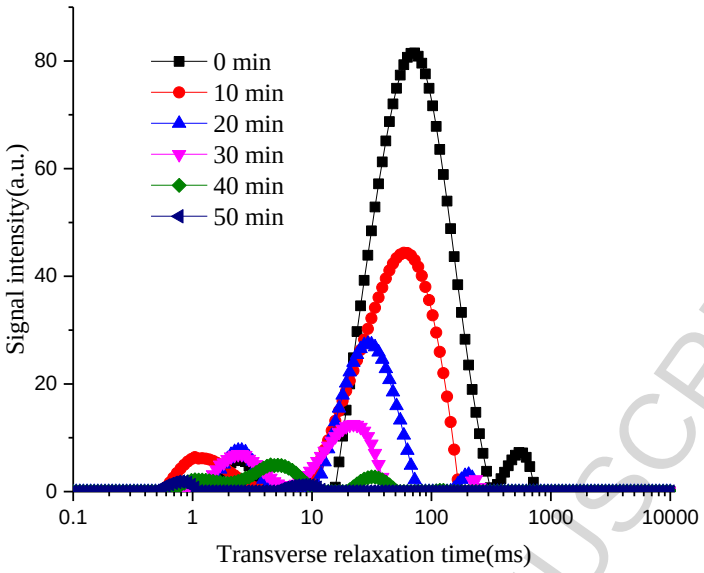

Fig 2. The transverse relaxation time (T_2) curves of the ginger cubes during MVD under 200 W microwave power.

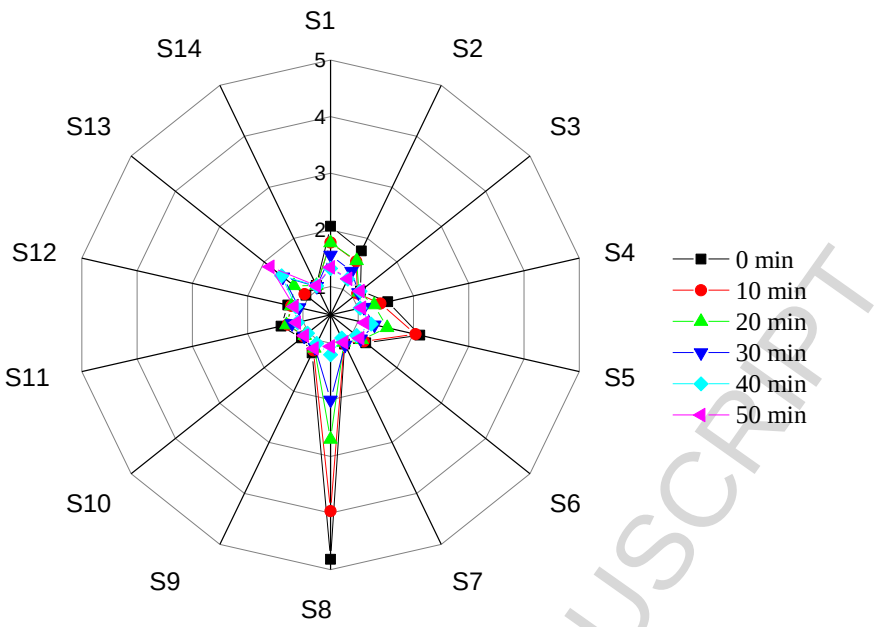

Fig 3. Radar chart of E-nose analysis of flavor of ginger under 200 W microwave power

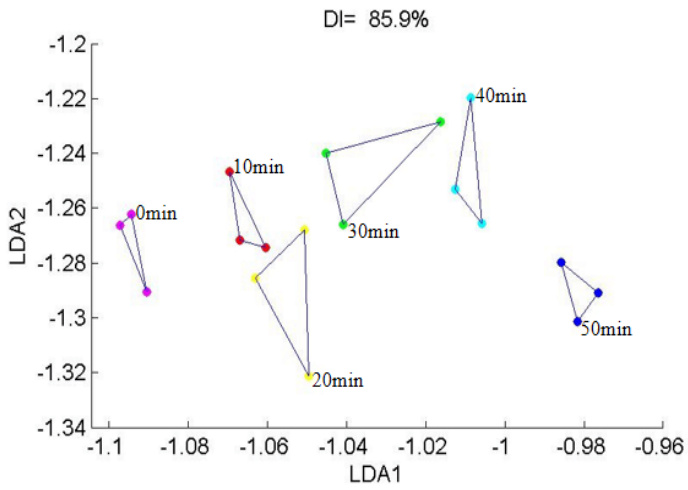

Fig 4. Linear Discriminant Analysis (LDA) chart of E-nose analysis of flavor of ginger

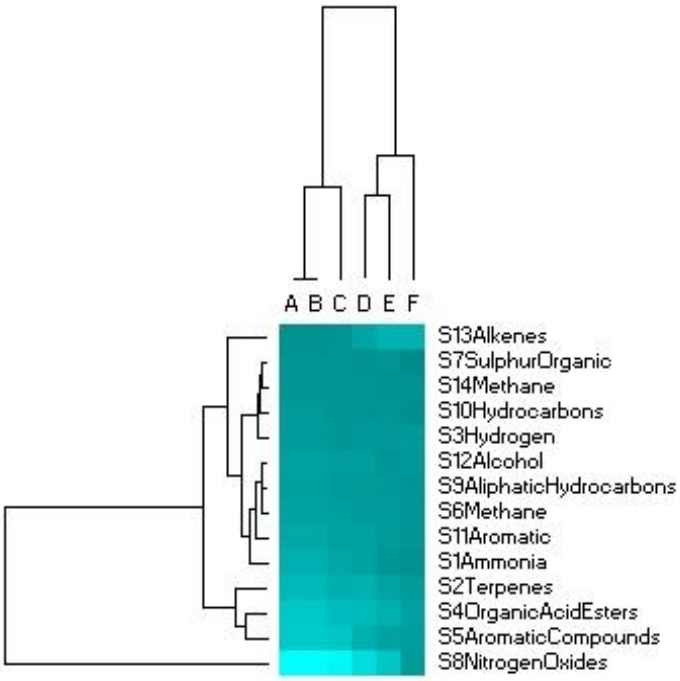

Fig 5. Hierarchical clustering analysis (HCA) chart of E-nose sensors analysis of flavor of ginger

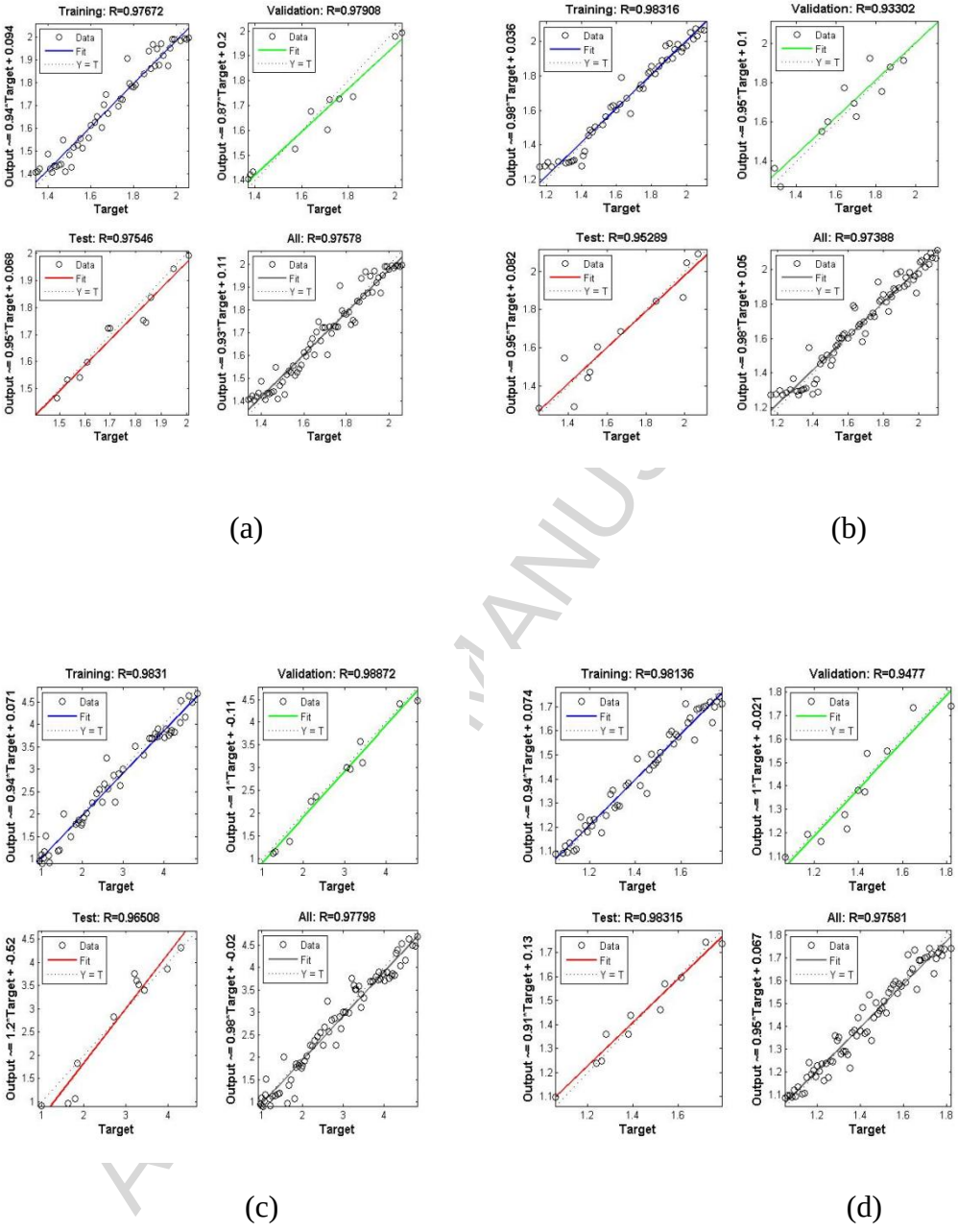

Fig 6. Establishment of prediction model by BP-ANN. (a) The prediction model of organic acid esters and terpenes (S_4); (b) The prediction model of alcohol (S_5); (c) The prediction model of nitrogen oxides (S_8); (d) The prediction model of alkenes (S_{13})

Table 1 Properties of sensor on MOS electronic nose

Sensor No.	General description
S1	Ammonia, used as sensor for aromatic compounds
S2	Reacts on sulphur compounds, H2S 1x10^4 g/L. Otherwise sensitive to many terpenes and sulphur organic compounds, which are important for smell, limonene, pyrazine
S3	Mainly hydrogen, selectively, (breath gases)
S4	Organic acid esters and terpenes, aromatic compounds, less polar compounds
S5	Detects alcohol's, partially aromatic compounds, broad range
S6	Sensitive to methane (environment) ca. 1x10^-2 g/L. Broad range
S7	Aromatics compounds, sulphur organic compounds
S8	Very sensitive, broad range sensitivity, react on nitrogen oxides
S9	Aliphatic hydrocarbons, aromatic compounds
S10	Hydrocarbons
S11	Aromatic compounds
S12	Alcohol, organic solvents
S13	Alkenes, aromatic compounds, less polar compounds
S14	Reacts on high concentrations >0.1 g/L, sometime very selective (methane)

Table 2 The volatile compounds of ginger with different drying times as detected by GC-MS

No	RT	Volatile compound	Relative content						
			fresh	**10 min**	**20 min**	**30 min**	**40 min**	**50 min**	**60 min**
Alkenes									
1	26.945	α- zingberene	14.96	14.99	15.35	16.66	16.87	17.02	17.21
2	32.623	α- farnesene	7.93	7.99	8.24	8.96	9.55	10.69	10.02
3	33.295	β-sesquiphellandrene	6.34	6.13	5.02	4.55	3.40	3.31	3.15
4	12.330	camphene	5.93	5.84	4.75	4.01	3.22	2.16	0.05
5	24.344	2,6-dimethyl-2, 6-octadiene	2.13	2.25	2.44	2.56	2.60	2.61	2.63
6	30.991	α-curcumene	1.52	1.50	1.42	1.04	0.85	0.70	0.64
7	24.126	α- pinene	0.24	0.30	1.22	1.38	1.55	1.64	1.58
8	13.235	myrcene	1.05	1.05	1.08	1.22	1.28	1.33	1.24
9	13.317	α-selinene	1.22	1.21	1.14	1.05	0.88	0.79	0.24
10	28.357	β-elemene	0.46	0.55	0.62	0.50	0.44	0.51	0.52
11	30.797	germacrene	0.88	0.83	0.72	0.66	0.51	0.55	0.53

12	15.976	4-carene	0.15	0.14	0.08	0.05	0.04	-	-
13	29.373	β-famesene	0.33	0.34	0.35	0.38	0.44	0.41	0.40
14	13.560	α-phellandrene	0.16	0.15	0.16	0.12	0.11	0.13	0.12
15	28.723	α- muurolene	0.17	0.18	0.20	0.26	0.25	0.28	0.29
16	14.951	(Z)-3,7-dimethyl-1,3,6-octatriene	0.15	0.16	0.18	0.25	0.36	0.38	0.39
17	14.001	α-terpinene	0.02	0.01	-	-	-	-	-
18	14.536	ocimene	0.14	0.16	0.28	0.55	0.59	0.67	0.63
19	11.857	β-pinene	1.46	1.40	1.05	0.55	0.32	0.28	0.27
20	17.122	alloocimene	0.08	0.09	0.09	0.11	0.13	0.14	0.15
21	29.086	α-gurjunene	0.06	0.07	-	-	-	-	-
22	14.015	2-carene	0.22	0.18	0.09	0.04	-	-	-
23	29.842	(+)-epi-bicyclosesquiphellandrene	0.02	0.02	-	-	-	-	-
24	29.670	alloaromadendrene	0.15	0.14	0.07	0.06	0.09	0.08	0.08
25	12.630	1,3,8-p-menthatriene	0.02	-	-	-	-	-	-
26	24.119	α-cubebene	0.09	0.09	0.10	0.15	0.11	0.13	0.12
27	283.114	germacrene-d	1.11	0.24	-	-	-	-	-
28	29.693	aromadendrene	0.16	-	-	-	-	-	-

29	29.070	β-guaiene	0.04	0.03		-	-	-	-
30	32.778	cyclohexene,3-(1,5-dimethyl-4-hexenyl)-6 - methylene	-	-	-	3.68	5.88	7.26	8.84
31	36.548	β-phellandren	-	-	-	3.75	5.43	6.01	6.28
alcohols									
32	14.337	eucalyptol	10.01	9.88	7.32	4.22	2.34	0.99	0.33
33	20.835	geraniol	5.96	4.90	3.68	1.55	1.08	0.73	0.38
34	18.993	α-terpineol	0.63	0.68	0.85	0.53	0.38	0.24	0.11
35	19.989	citronellol	0.53	0.54	0.67	0.57	0.55	0.58	0.50
36	16.367	linalool	0.40	0.36	0.35	0.28	0.26	0.22	0.20
37	18.295	2-camphanol	0.30	0.28	0.28	0.14	0.11	0.09	0.08
38	35.409	Nerolidol	0.21	0.23	0.26	0.37	0.41	0.45	0.44
39	34.608	elemol	0.13	0.13	0.13	0.17	0.18	0.19	0.20
40	35.912	germacrene D-4-ol	0.07	0.06	-	-	-	-	-
41	15.468	β-terpineol	0.06	0.05	-	-	-	-	-
42	26.337	Bergamotol, Z-α-trans-	-	-	0.37	0.42	0.55	0.61	0.69
43	33.421	homovanillyl alcohol	-	-	-	-	-	0.08	0.14
44	35.576	6-octen-1-yn-3-ol,3,7-dimethyl	-	-	-	-	-	0.10	0.10
aldehyde									

45	21.345	(E)-citral	7.83	7.84	7.01	5.22	3.14	1.21	0.35
46	20.338	(Z)-citral	1.40	1.38	1.30	1.05	0.62	0.39	0.28
47	17.791	citronellal	0.23	0.21	0.08	-	-	-	-
48	19.199	decanal	0.07	0.22	0.05	-	-	-	-
49	20.801	(E)-2-decenal	0.08	0.35	-	-	-	-	-
50	25.334	2,6-octadienal, 3,7-dimethyl	-	1.56	1.78	1.85	2.69	3.04	3.27
51	26.870	3-hydroxy-2-methylbenzaldehyde	-	-	-	-	0.14	0.21	0.23
Ketones									
52	21.945	2-undecanone	0.04	0.08	0.27	0.56	0.93	0.99	1.05
Esters									
53	26.260	geranyl acetate	22.74	23.81	26.43	30.08	32.44	34.16	28.51
54	14.673	heptyl acetate	0.35	0.31	0.22	0.14	0.08	-	-
55	14.673	L-bornyl acetate	0.63	0.60	0.41	0.24	0.07	-	-
56	24.875	nerolyl acetate	0.36	0.54	0.67	1.86	2.04	2.22	2.34
57	23.164	myrtenyl acetate	0.17	0.15	0.08	0.02	-	-	-
58	19.434	octyl acetate	0.18	0.15	0.04	-	-	-	-
59	27.586	bornyl acetate	-	-	-	1.02	1.15	1.27	1.38

	A_{21}	A_{22}	A_{23}	A_{Total}	S_4	S_5	S_8	S_{13}
A_{21}	1	0.872**	0.201	0.156	0.487	0.304	0.664*	0.344
A_{22}		1	-0.198	0.359	0.556*	0.116	-0.217	0.185
A_{23}			1	0.962**	0.803**	0.867**	0.841**	-0.803**
A_{Total}				1	0.955**	0.921**	0.826**	-0.954**
S_4					1	0.905**	0.893**	-0.913**
S_5						1	0.754**	-0.647*
S_8							1	-0.885**
S_{13}								1

Table 3 Correlation analysis between electronic nose sensors and NMR parameters.

**$P < 0.01$ Correlation is significant at the 0.01 level.

*$P < 0.05$ Correlation is significant at the 0.05 level.

Table 4 Performance of different flavor prediction models

Model	**MSE(10^{-2})**	**True value**	**Predicted value**	**R^2**
S4	0.0952	1.0422	1.0820	0.9571
		1.1833	1.1903	
		1.2542	1.2098	
		1.3651	1.3509	
S5	1.1236	1.1206	1.0388	0.9494
		1.5644	1.5922	
		1.8329	1.6698	
		2.1133	2.2176	
S8	4.7468	1.0443	1.0972	0.9720
		2.3309	2.1511	
		3.6454	3.4498	
		4.4738	4.5901	
S13	0.4898	1.0551	1.0532	0.9542
		1.3304	1.4016	
		1.7108	1.5903	
		1.8544	1.8542	

MSE Mean Square Error, R^2 coefficient of determination

Highlights:

- LF-NMR and electronic nose combined with GC-MS were used to collect the data of moisture state and volatile substances.
- LDA and HCA analysis confirmed the electronic nose characteristic sensor data S_4, S_5, S_8 and S_{13} corresponded with the data measured by GC-MS.
- The correlation analysis showed LF-NMR parameters and characteristic sensors were significantly correlated.
- The results of the BP-ANN prediction showed that the model fitted well and had strong approximation ability ($R>0.95$ and error<3.65%) and stability.